

Influence of Collisions on Parametric Instabilities Induced by Lower Hybrid Waves in Tokamak Plasmas

C. Castaldo¹, A. Di Siena², R. Fedele², F. Napoli³,
L. Amicucci¹, R. Cesario¹, G. Schettini⁴

¹*ENEA, Unità Tecnica Fusione, C.R. ENEA Frascati, CP65, 00044 Frascati, Italy*

²*Dipartimento di Fisica, Università Federico II and INFN, Napoli, Italy*

³*Lancaster University, Engineering Department, Lancaster, United Kingdom*

⁴*Università degli Studi Roma Tre, Dipartimento di Ingegneria, Roma, Italy*

Abstract. Parametric instabilities induced at the edge by lower hybrid wave power externally coupled to tokamak plasmas have, via broadening of the antenna spectrum, strong influence on the power deposition and current drive in the core. For modeling the parametric instabilities, the effect of the collisions has been neglected so far. In the present work, a collisional parametric dispersion relation is derived for the first time in the frame of a kinetic model. Numerical solutions show that in the cold plasma region near the antenna mouth the collisions prevent the onset of the parametric instabilities. This result is important for present lower hybrid current drive experiments, as well as to assess the feasibility of the lower hybrid current drive concept in fusion reactor scenarios.

1. Introduction

Lower hybrid waves, coupled to tokamak plasmas by microwave power utilising phased waveguide arrays launchers, efficiently produces a non-inductive plasma current in tokamak plasmas [1, 2]. Successful exploitation of the lower hybrid current drive (LHCD) effect was demonstrated to occur at reactor relevant, high plasma densities [3]. The LHCD, in addition to the bootstrap current [4], can provide a fully active control of the current density profiles [5]. This goal is essential for fusion reactors, since it allows to achieve sufficient stability and energy confinement of the plasma column and extend towards steady state operations the duration of the plasma current that is intrinsically transient in tokamaks.

In fusion reactors scenarios, such as ITER or DEMO, the radial profiles of the LHCD power deposition and current drive can be controlled by the injected power and by two parameters of the coupled power spectrum vs. the refractive index parallel to the static magnetic field, namely the peak value $N_{//0}$, and the width $\Delta N_{//0}$ of the main lobe [5]. These are determined, following the linear theory, only by the phasing of the waveguide array launcher, which can be varied electronically during the radiofrequency (rf) pulse. Thus, the LHCD can be added to the bootstrap current providing an efficient and flexible tool to produce and control in real time steady-state fusion scenarios by means of a high fraction of non-inductive current.

It is worth noting that other available tools to drive a non-inductive plasma current in tokamaks, namely the rf power injection in the ion or electron cyclotron range of frequency as well as the neutral beam injection, do not have so far produced, in the outer radial half of plasma, plasma currents with an efficiency and flexibility of deposition comparable to LHCD. This goal is necessary for actively controlling the safety factor profile in order to access to reactor relevant regimes. To obtain this control LHCD still remains the ideal method, in combination with the bootstrap current.

However, a limit of the LHCD concept might be the occurrence of nonlinear phenomena, which can modify the coupled power spectrum in the parallel refractive index and, possibly, prevent the LH wave power penetration in the plasma core.

Lack of rf power penetration, attributed to nonlinear effects [6], already occurred in the early LH experiments in tokamaks, aimed at testing the ion heating in the plasma core predicted by the theory [7,8]. For enabling the mode conversion of the LH waves into hot ion modes and produce ion heating, such experiments operated at relative high plasma density (line-averaged value $n_{e,av} \sim 1.5 \cdot 10^{20} \text{ m}^{-3}$). In these conditions, only strong, parametric instabilities (PI) at the edge were observed [9]. The typical signature of this nonlinear effect, as detected by rf probes, consists in a large broadening (up to about 40 MHz) at around the operating line f_o . The rf spectra are asymmetric, i.e. dominated by sidebands that are down-shifted with respect to f_o . Sidebands shifted by harmonics of the ion cyclotron frequency were also observed. Modeling based on the PI theory [10] provided an interpretation of the rf spectra obtained during the early LH experiments aimed at heating the plasma ions [6,11].

In LHCD experiments, operating at low plasma density (up to line-averaged value $n_{e,av} \sim 0.4 \cdot 10^{20} \text{ m}^{-3}$), PI are also observed, but are comparably weak [12] and the rf power does penetrate in the plasma core, successfully driving a plasma current [13]. In such scenarios, no significant depletion of the injected power by PI is expected [14]. It has been pointed out, however, that the observed broadening of the frequency spectrum due to PI is also accompanied by a significant broadening of the spectrum in the parallel refractive index [15]. A full wave analysis of the propagation of a LH wave power pulse, performed in the frame of nonlinear fluid theory also predicted a spectral broadening $\Delta N_{\parallel}/N_{\parallel}$ of the order of unity for typical LH and plasma parameters [16]. Such spectral broadening, which occurs at the edge of the plasma column, has a profound effect on the LHCD physics, concerning the power absorption and current drive in the plasma core. The latter are indeed based on the LH wave interaction at the Landau resonance $N_{\parallel} = c/v_{\parallel}$ with a significant fraction of the plasma electrons, as given by the distribution function $f(v_{\parallel})$ in the velocity along the static magnetic field.

Based on the numerical code LH^{star}, which is up to now the only tool able to calculate the LH power deposition and the driven current density profiles taking into account the effects of PI, it was shown that the spectral broadening represents an important contribution in bridging the N_{\parallel} gap in LHCD [17,18]. The spectral gap problem in LHCD physics consists in explaining the mechanisms that broaden and up-shift the launched power spectrum in N_{\parallel} . A redistribution in the N_{\parallel} spectrum coupled by LH antennas, as given by the linear theory of the ‘LH grill’ (developed since the early ’70 [19]), is necessary for justifying the power absorption and the amount of current driven in the experiments, which should be otherwise negligible.

A more remarkable success of the LHCD modeling taking into account the effects of PI is the prediction, confirmed by the experiments, that LHCD approaching reactor-graded high plasma densities can have success provided that a relatively high electron temperature in the outer plasma should be produced [3]. This allow to overcome the density limit observed in LHCD experiments, namely a threshold of the line-averaged density above which the current driven by the rf power injection becomes much lower than expected by the LHCD theory and sharply disappear (see the review of LHCD experiments by F. De Marco in [20]). The density limit occurs when the edge density approach the values typical of the early LH experiment aimed at ion heating and required by fusion reactors scenarios.

This suggests that the same nonlinear effects are present, making questionable the use of LHCD. However, as anticipated above, important evidences of LH power penetration in the plasma core were obtained in the FTU tokamak at reactor relevant central plasma density $n_{e,o} \approx 5 \cdot 10^{20} \text{ m}^{-3}$ with suitable plasma operations, e.g. performing wall lithisation or injecting pellets to increase the core plasma density without perturbing the edge. These operations allowed to keep the edge electron temperature sufficiently high, even at reactor-graded plasma density, that the PI induced spectral broadening in the frequency domain was $\Delta f_{40}/f_o < 1\%$. Here Δf_{40} is the spectral width at -40 dB from the peak and $f_o = 8.0 \text{ GHz}$ is the operating frequency of the rf source. Conversely, in normal FTU plasma discharge operations, at even lower central plasma density $n_{e,o} \approx 3 \cdot 10^{20} \text{ m}^{-3}$, the observed spectral broadening was a factor two larger and no LH wave-paricle interactions in the plasma core has been observed.

The observation of LH interaction with core plasma electrons well above the LHCD density limit [3] thus represents a breakthrough, which reopen the exploration of LH ion heating scenarios and raises the chances for a profitable use of LHCD in fusion reactors.

The importance of the nonlinear spectral broadening for a proper design of the LHCD system in fusion reactors motivates an effort to improve the modeling of PI. Here we discuss, for the first time, the influence of the collisions on PI induced by LH power waves, which are neglected in the standard modeling. The role of the collisions on PI induced by LH power waves, expecially near the antenna mouth, can be anticipated as significant observing that in such relative cold ($T_e \leq 10 \text{ eV}$) and dense plasma ($n_e \sim 10^{18} \text{ m}^{-3}$) the electron-electron collision rates are of the same order of the frequency of the ion-acoustic quasi-modes. The latter are involved in the main channel of the PI induced by LH power waves in current drive experiments.

The standard modeling of PI [18,21] is based on the calculation of the growth rates of the instabilities, given by local solutions of the parametric dispersion relation (PDR). The PDR is derived in the framework of the kinetic theory [10], assuming collisionless plasmas and utilising the electrostatic approximation. Four waves interaction is considered, involving three high frequency (hf, GHz range) modes, namely the injected LH *pump* wave and two LH sidebands at lower and higher frequency, emerging from the thermal noise, and a resonant mode or quasi-mode at low frequency (lf, MHz range). The growth rates of the most unstable LH sidebands are used to evaluate their space amplification in steady state conditions, taking into account the finite area illuminated by the injected LH pump waves as well as the convective losses due to the plasma inhomogeneity, on the basis of the eikonal theory.

In this paper we suggest that the PI modeling should incorporate a new PDR, taking into account the influence of the collisions. We show indeed that the collisions have a strong effect on the growth rates of the LH sidebands and can possibly suppress the PI.

In Section 2, the new PDR, involving the collisional effects, is derived on the basis of a kinetic model and using a perturbative approach. Numerical solutions of such parametric dispersion equations are discussed in Section 3. Here a parametric study of the growth rates of the instabilities is proposed, considering the effects of different plasma and rf parameters. The results obtained are then summarized in Section 4, mainly concerning their relevance in present LHCD experiments and in fusion reactors scenarios.

2. Collisional parametric dispersion equation

We derive here a collisional parametric dispersion equation useful to evaluate the growth rates of PI induced by LH wave power in the plasma region in front of the LH antenna mouth. Uniform and stationary plasma model is used, with cartesian axis Z aligned along the static magnetic field $\mathbf{B}_0 = B_0 \mathbf{z}$. The basic equations are given by the self-consistent system of the Maxwell equations coupled to the Boltzmann kinetic equation for the single particle distribution functions f_α . A particle conserving BGK collision operator [22] is used as an approximate model of the collision integral,

$$\left(\frac{\partial f_\alpha}{\partial t}\right)_{coll} \cong -\nu_\alpha [f_\alpha - f_\alpha^o(n_\alpha/n_\alpha^o)] \quad (1)$$

where f_α^o is the unperturbed, local equilibrium and ν_α are characteristic relaxation rates. We adopt this simple model, as it seems fully adequate to predict collisional effects in kinetic models of wave propagation [23]. When $T_i \approx T_e$ and single ionized atoms are considered, the relaxation rates can be approximated by the following expressions [24]: $\nu_{e,HZ} = 2.9 \cdot 10^{-6} \lambda_C n_e T_e^{-3/2}$, $\nu_{i,HZ} = 4.8 \cdot 10^{-8} \lambda_C n_e T_i^{-3/2} \mu_i^{-1/2}$. Here the relaxation rates for the electrons (subscript e) and the ions (subscript i) are given in Hz, the temperatures $T_{e,i}$ are in eV, the plasma density n_e is in cm^{-3} , μ_i is the ion mass in units of the proton mass and λ_C is the Coulomb logarithm. We observe that the ion relaxation rates are two order of magnitude lower than the electron collision rates. As a result, we have found that the introduction of the collision effects into the ion kinetic equation has a negligible effect on the solutions of the parametric dispersion relation.

We assume that the local equilibria are given by the Maxwellians $f_\alpha^o = n_\alpha^o (\pi v_{th,\alpha})^{-3/2} \exp[-(|\mathbf{v}|/v_{th,\alpha})^2]$. The thermal velocity is defined here as $v_{th,\alpha} = \sqrt{2k_B T_\alpha / m_\alpha}$, T_α is the local temperature of the species α considered, with mass m_α and electric charge q_α , k_B is the Boltzmann's constant and $n_\alpha = \int d^3\mathbf{v} f_\alpha$ is the number density. We assume that the quasi-neutrality condition $\sum_\alpha q_\alpha n_\alpha^o = 0$ is fulfilled.

We consider LHCD experimental scenarios such that the dominant nonlinear effects produce sideband LH waves only in a narrow hf range $[f_o - \Delta f, f_o + \Delta f]$, with $\Delta f \ll f_{c,i}$, around the peak frequency f_o of the injected LH wave power. Here $f_{c,i}$ indicates the cyclotron frequency of the ion species. In such scenarios, the main parametric instability channel is provided by ion acoustic quasi-modes, with frequency $f \leq \Delta f$, which are excited by the nonlinear beating of the LH waves [21]. The scaling $\Delta f \ll f_{c,i} \ll f_o \ll f_{c,e}$, where $f_{c,e}$ is the cyclotron frequency of the electrons, allows a greater simplification of the kinetic equation. In the hf range the plasma ions can be considered as completely unmagnetised, i.e. the magnetic force can be neglected in the kinetic equation. However, for the sake of simplicity, we further assume that in the hf range the plasma ions are fixed, i.e. we neglect the hf perturbations of their distribution functions. This assumption is justified by the observation that in the plasma region near the antenna mouth the ion contribution to the linear LH dispersion equation is negligible.

The plasma electrons and, in the lf range, the plasma ions can be considered as completely magnetized, i.e. their motion can be represented by the 1D motion of their guide center along the direction of the magnetic field. We observe that in the cold plasma region near the LH antenna mouth is well verified the condition $k_{\perp}\rho_i \ll 1$. Here k_{\perp} is the wavenumber of any of the relevant modes or quasi-modes involved in the PI and ρ_i is the ion Larmor radius. Therefore, considering also the above frequency scaling, the dynamics of the plasma particles can be approximated by the motion parallel to the magnetic field in both the high frequency (magnetized electrons, fixed ions) and low frequency (magnetized electrons and ions) regimes.

At this regard, we observe that in the plasma region near LH antennas, with typical kinetic parameters $T_e \leq 10$ eV and $n_e \leq 5 \cdot 10^{18} \text{ m}^{-3}$, the motion parallel to the magnetic field has been indeed recognized as the dominant dynamics concerning the standard collisionless parametric dispersion equation [21,25,26]. Consequently, we can assume that in the velocity space, the distribution functions have cylindrical symmetry around the axis of the velocities parallel to the magnetic field. Application of the integral operator $\mathcal{J}_{\perp} = \iint dv_x dv_y$ to the Boltzmann equation, thus gives the kinetic equation

$$\frac{\partial g_{\alpha}}{\partial t} + v_z \frac{\partial g_{\alpha}}{\partial z} + \frac{q_{\alpha}}{m_{\alpha}} E_z \frac{\partial g_{\alpha}}{\partial v_z} = -\nu_{\alpha} [g - g_{\alpha}^o(n_{\alpha}/n_{\alpha}^o)] \quad (2),$$

where $g_{\alpha}(t, z, v_z) = \mathcal{J}_{\perp}[f_{\alpha}]$ and $g_{\alpha}^o(v_z) = \mathcal{J}_{\perp}[f_{\alpha}^o]$.

We use the spectral method and the perturbation theory to solve the self-consistent system obtained coupling the above equation to the Maxwell equations.

The expansion parameter is $\varepsilon = e|E_{z,o}|/m_e\omega_o v_{th,e} \ll 1$, where e is the elementary charge, $|E_{z,o}|$ is the maximum amplitude of the z -component of the rf electric field, and $\omega_o = 2\pi f_o$ is the peak angular frequency of the injected rf wave power.

The first and second order perturbations of the distribution functions are given by

$$g_{\alpha;\omega,k}^{(1)} = \frac{i}{\omega + iv_{\alpha} - k_z v_z} \left[\frac{n_{\alpha;\omega,k}^{(1)}}{n_{\alpha}^{(o)}} v_{\alpha} g_{\alpha}^o - \frac{q_{\alpha}}{m_{\alpha}} E_{z;\omega,k} \frac{\partial g_{\alpha}^{(o)}}{\partial v_z} \right] \quad (3)$$

$$g_{\alpha;\omega,k}^{(2)} = \frac{i}{\omega + iv_{\alpha} - k_z v_z} \left[\frac{n_{\alpha;\omega,k}^{(2)}}{n_{\alpha}^{(o)}} v_{\alpha} g_{\alpha}^o - \frac{q_{\alpha}}{m_{\alpha}} \sum_{\omega',k'} E_{z;\omega-\omega',k-k'} \frac{\partial g_{\alpha;\omega',k'}^{(1)}}{\partial v_z} \right] \quad (4)$$

The nonlinear terms here considered involve only the beating of the electric field associated with the injected LH pump wave with the electric field of a lf mode or quasi-mode, or the hf electric field of a LH sideband. Other nonlinear beating terms are neglected. This approximation is justified if the pump depletion is negligible and the amplitude of the electric field of LH the pump wave is much larger than the amplitude of the electric field of the LH sidebands and the lf modes or quasi-modes.

We can now evaluate self-consistently the electric fields of the hf and lf modes, by application of the perturbation theory and the spectral analysis to the wave equation derived from the Maxwell equations. To this end we need to calculate the spectral components of the perturbed charge and current densities, at the first and second order in the expansion parameter ε (at the zero order the total charge density and the total current density are zero).

We note that, owing to the use of a particle conserving collision integral, for each plasma species α , the continuity equation $\nabla \cdot \mathbf{j}_\alpha^{(m)} + \partial_t \rho_\alpha^{(m)} = 0$ holds at any order m of the perturbation. The perpendicular components of the current density perturbation are zero, due to the assumed cylindrical symmetry of the distribution functions. The continuity thus follows from the identity

$$k_z j_{\alpha,z;\omega,\mathbf{k}}^{(m)} = \omega \rho_{\alpha;\omega,\mathbf{k}}^{(m)} \quad (5),$$

where $\rho_{\alpha;\omega,\mathbf{k}}^{(m)} = q_\alpha n_{\alpha;\omega,\mathbf{k}}^{(m)} = q_\alpha \int d\mathbf{v}_z g_{\alpha;\omega,\mathbf{k}}^{(m)}$ and $j_{\alpha,z;\omega,\mathbf{k}}^{(m)} = q_\alpha \int d\mathbf{v}_z v_z g_{\alpha;\omega,\mathbf{k}}^{(m)}$.

Taking into account the continuity equations we thus obtain the following wave equation, retaining nonlinear terms up to the second order:

$$\left(\frac{\omega^2}{c^2} - k^2\right) E_{z;\omega,\mathbf{k}} = \frac{4\pi i}{k_z} \left(k_z^2 - \frac{\omega^2}{c^2}\right) \sum_\alpha \left[\rho_{\alpha;\omega,\mathbf{k}}^{(1)} + \rho_{\alpha;\omega,\mathbf{k}}^{(2)}\right] \quad (11)$$

In the *hf* range, the ions are assumed fixed and only the electron density perturbation should be considered. The nonlinear term $\rho_{e;\omega,k_y,k_z}^{(2)}$ is produced by the beating of the toroidal components of the *hf* pump wave and *lf* electric fields, as given in Eq. (4). In the *lf* range, the ion contribution is important, but limited to the linear perturbation of the charge density. Due to their large inertial mass, the ion species contributions to the nonlinear perturbation of the charge density can be only due to the beating of *lf* fields and, therefore, can be neglected.

The first and second order number density perturbations are obtained from Eq. (3) and Eq. (4) by integration in the velocity 1D space, taking into account the Landau prescription:

$$n_{\alpha;\omega,\mathbf{k}}^{(1)} = -2i \frac{q_\alpha}{m_\alpha} \frac{n_\alpha^{(o)}}{k_z v_{th,\alpha}^2} E_{z;\omega,\mathbf{k}} \frac{1 + \zeta_\alpha Z(\zeta_\alpha)}{1 + i\gamma_\alpha Z(\zeta_\alpha)} \quad (12)$$

$$n_{\alpha;\omega,\mathbf{k}}^{(2)} = \frac{\omega_\alpha^2}{2\pi m_\alpha v_\alpha^4} \sum_{\omega',\mathbf{k}'} E_{z;\omega-\omega',\mathbf{k}-\mathbf{k}'} E_{z;\omega',\mathbf{k}'} (k_z k_z')^{-1} F_c(\zeta_\alpha, \zeta'_\alpha, s, s') \quad (13)$$

Here $Z(\zeta)$ is the plasma dispersion function, ω_α is the plasma frequency of the species α , $\zeta_\alpha \equiv (\omega + i\nu_\alpha)/(|k_z|v_{th,\alpha})$, $\gamma_\alpha \equiv \nu_\alpha/(|k_z|v_{th,\alpha})$.

The coupling function $F_c(\zeta_\alpha, \zeta'_\alpha, s, s')$, involved in the nonlinear beating terms, is given by the following equations:

$$F_c(\zeta_\alpha, \zeta'_\alpha, s, s') \equiv [F_a(\zeta_\alpha, \zeta'_\alpha, s, s') + F_b(\zeta_\alpha, \zeta'_\alpha, s, s')]/[1 + i\gamma_\alpha Z(\zeta_\alpha)] \quad (14)$$

$$F_a(\zeta_\alpha, \zeta'_\alpha, s, s') \equiv \frac{s' C_1(\zeta'_\alpha) - s C_1(\zeta_\alpha)}{s \zeta_\alpha - s' \zeta'_\alpha} - \frac{s \zeta_\alpha [s' C_1(\zeta'_\alpha) + s Z(\zeta_\alpha)] - 2 \zeta_\alpha'^2 C_2(\zeta'_\alpha)}{(s \zeta_\alpha - s' \zeta'_\alpha)^2} \quad (15)$$

$$F_b(\zeta_\alpha, \zeta'_\alpha, s, s') \equiv \frac{is'\gamma'_\alpha C_2(\zeta'_\alpha)}{[1 + i\gamma'_\alpha Z(\zeta'_\alpha)]} \left[\frac{sZ(\zeta_\alpha) - s'Z(\zeta'_\alpha)}{(s\zeta_\alpha - s'\zeta'_\alpha)^2} + \frac{2C_2(\zeta_\alpha)}{s\zeta_\alpha - s'\zeta'_\alpha} \right] \quad (16)$$

with $s \equiv \text{sign}(k_z)$, $C_1(\zeta) \equiv 2\zeta[1 + \zeta Z(\zeta)] - Z(\zeta)$, $C_2(\zeta) \equiv 1 + \zeta Z(\zeta)$.

We consider here four waves interaction, involving the injected LH pump wave (subscript 0) two LH sidebands at lower (subscript 1) and higher (subscript 2) frequency, and a resonant mode or quasi-mode at low frequency (no subscript).

The relevant selection rules for such interaction are $\omega_1 = \omega - \omega_o$, $\mathbf{k}_1 = \mathbf{k} - \mathbf{k}_o$, $\omega_2 = \omega + \omega_o$, $\mathbf{k}_2 = \mathbf{k} + \mathbf{k}_o$. The following field equations are thus obtained from Eq. (11), (12) and (13):

$$\begin{aligned} \varepsilon_1^{hf} E_{z,1} = & i \frac{\varepsilon}{|E_{z,o}|} \left(1 - \frac{\omega_1^2}{c^2 k_{z,1}^2} \right) E_{z,o}^* E_z \left[\frac{F_c(\zeta_{e1}, \zeta_e, s_1, s)}{\xi} - \frac{F_c(\zeta_{e1}, \zeta_{eo}, s_1, -s_o)}{\xi_o} \right] \\ & + i \frac{\varepsilon}{|E_{z,o}|} \left(1 - \frac{\omega_1^2}{c^2 k_{z,1}^2} \right) E_{z,o} E_z^* \left[\frac{F_c(\zeta_{e1}, \zeta_{eo}, -s_1, s_o)}{\xi_o} - \frac{F_c(\zeta_{e1}, \zeta_{eo}, -s_1, -s)}{\xi} \right] \quad (17) \end{aligned}$$

$$\begin{aligned} \varepsilon_2^{hf} E_{z,2} = & i \frac{\varepsilon}{|E_{z,o}|} \left(1 - \frac{\omega_2^2}{c^2 k_{z,2}^2} \right) E_{z,o}^* E_z \left[\frac{F_c(\zeta_{e2}, \zeta_e, s_2, s)}{\xi} + \frac{F_c(\zeta_{e2}, \zeta_{eo}, s_2, s_o)}{\xi_o} \right] \\ & - i \frac{\varepsilon}{|E_{z,o}|} \left(1 - \frac{\omega_2^2}{c^2 k_{z,2}^2} \right) E_{z,o} E_z^* \left[\frac{F_c(\zeta_{e2}, \zeta_e, -s_2, -s)}{\xi} + \frac{F_c(\zeta_{e1}, \zeta_{eo}, -s_2, -s_o)}{\xi_o} \right] \quad (18) \end{aligned}$$

$$\begin{aligned} \varepsilon^{lf} E_z = & i \frac{\varepsilon}{|E_{z,o}|} \left(1 - \frac{\omega^2}{c^2 k_z^2} \right) E_{z,o}^* E_{z,2} \left[\frac{F_c(\zeta_e, \zeta_{e2}, s, s_2)}{\xi_2} - \frac{F_c(\zeta_e, \zeta_{eo}, s, -s_o)}{\xi_o} \right] \\ & + i \frac{\varepsilon}{|E_{z,o}|} \left(1 - \frac{\omega^2}{c^2 k_z^2} \right) E_{z,o} E_{z,1} \left[\frac{F_c(\zeta_e, \zeta_{eo}, s, s_o)}{\xi_o} + \frac{F_c(\zeta_e, \zeta_{e1}, s, s_1)}{\xi_1} \right] \quad (19) \end{aligned}$$

Here we define the parameters $\xi \equiv k_z v_{th,e} / \omega_o$ and $\xi_h \equiv k_{zh} v_{th,e} / \omega_o$ (with $h=0,1,2$). The linear dispersion functions of hf fields ε_j^{hf} (with $j=1,2$) and the linear dispersion function of the lf field ε^{lf} are given by the following equations:

$$\varepsilon_j^{hf} = k_j^2 \lambda_{De}^2 \left(1 - \frac{\omega_j^2}{c^2 k_j^2} \right) + \left(1 - \frac{\omega_j^2}{c^2 k_j^2} \right) \frac{1 + \zeta_{ej} Z(\zeta_{ej})}{1 + i\gamma_{ej} Z(\zeta_{ej})} \quad (20)$$

$$\varepsilon^{lf} = k^2 \lambda_{De}^2 \left(1 - \frac{\omega^2}{c^2 k^2} \right) + \left(1 - \frac{\omega^2}{c^2 k^2} \right) \sum_{\alpha} \frac{1 + \zeta_{\alpha} Z(\zeta_{\alpha})}{1 + i\gamma_{\alpha} Z(\zeta_{\alpha})} \frac{\lambda_{De}^2}{\lambda_{D\alpha}^2} \quad (21)$$

In conclusion, the LH parametric dispersion relation (PDR), including the effects of the collisions, is obtained by Eq. (17), (18) and (19):

$$\varepsilon^{lf} = \frac{\mu_1}{\varepsilon_1^{hf}} + \frac{\mu_2}{\varepsilon_2^{hf}} \quad (22)$$

The parameters μ_1 and μ_1 are defined here as follows:

$$\mu_1 = \varepsilon^2 \left(1 - \frac{\omega_1^2}{c^2 k_{z1}^2} \right) \left[\frac{F_c(\zeta_{e1}, \zeta_e, s_1, s) F_c(\zeta_e, \zeta_{e0}, s, s_0)}{\xi \xi_0} - \frac{F_c(\zeta_{e1}, \zeta_{e0}, s_1, -s_0) F_c(\zeta_e, \zeta_{e0}, s, s_0)}{\xi_0^2} + \frac{F_c(\zeta_{e1}, \zeta_e, s_1, s) F_c(\zeta_e, \zeta_{e1}, s, s_1)}{\xi \xi_1} - \frac{F_c(\zeta_{e1}, \zeta_{e0}, s_1, -s_0) F_c(\zeta_e, \zeta_{e1}, s, s_1)}{\xi_0 \xi_1} \right] \quad (23)$$

$$\mu_2 = \varepsilon^2 \left(1 - \frac{\omega_1^2}{c^2 k_{z2}^2} \right) \left[\frac{F_c(\zeta_{e2}, \zeta_e, s_2, s) F_c(\zeta_e, \zeta_{e2}, s, s_2)}{\xi \xi_2} + \frac{F_c(\zeta_{e2}, \zeta_{e0}, s_2, s_0) F_c(\zeta_e, \zeta_{e2}, s, s_2)}{\xi_0 \xi_2} - \frac{F_c(\zeta_{e2}, \zeta_e, s_2, s) F_c(\zeta_e, \zeta_{e0}, s, -s_0)}{\xi \xi_0} - \frac{F_c(\zeta_{e2}, \zeta_{e0}, s_2, s_0) F_c(\zeta_e, \zeta_{e0}, s, -s_0)}{\xi_0^2} \right] \quad (24)$$

It can be shown that the collisional PDR, derived above, in the limit $\nu_\alpha \rightarrow 0$, tends to the standard non-collisional parametric dispersion equation obtained retaining only the dynamics parallel to the static magnetic field and neglecting the ion susceptibility in the hf dielectric function. We have verified that the numerical solutions of the Eq. (22), with $\nu_\alpha = 0$, are in reasonable agreement (within 10-20%) with the solutions of the standard PDR, as calculated by the relevant routine in the LH^{star} code.

3. Growth rates of PI induced by LH waves in collisional plasmas

In this section, we propose a parametric analysis of the stability of the LH sidebands coupled to LH power waves in collisional plasmas, based on numerical solutions of the new PDR, Eq. (22). The latter can be cast in the form $f_{PD}(\omega, k_\parallel, k_\perp, \delta, \omega_o, k_{\parallel,o}, \varepsilon, \sigma) = 0$, where f_{PD} is the parametric dispersion function, which is defined by $f_{PD} = 1 - (\mu_1/\varepsilon_1^{hf} + \mu_2/\varepsilon_2^{hf})/\varepsilon^{lf}$, the subscripts ‘ \parallel ’ and ‘ \perp ’ refer, respectively, to the directions parallel and perpendicular to the static magnetic field, $\delta = \angle(\mathbf{k}_\perp, \mathbf{k}_{\perp,o})$ and σ indicates the plasma parameters (density, temperatures of the electron and ion species and plasma composition). For fixed values of the subset of parameters $\{k_\parallel, k_\perp, \delta, \omega_o, k_{\parallel,o}, \varepsilon, \sigma\}$, the solution of the PDR thus consists of finding the zeros of the complex function f_{PD} of the complex variable ω . The imaginary part γ of such zeros is identical to the imaginary parts of $\omega_{1,2}$ and discriminates stable ($\gamma < 0$) and unstable ($\gamma > 0$) LH modes.

The algorithm implemented by a numerical code to find the zeros of the analytic dispersion function f_{PD} is based on the methods described in Ref. [27]. As a reference set of rf and plasma parameters in our analysis we use the values reported in Table I, which correspond to typical LHCD experiments in the FTU tokamak.

In order to identify the most unstable modes we find the maximum value of γ with respect to k_{\perp} and δ .

In Fig. 1 we plot the numerical values of ω and γ normalized to ω_o , the angular frequency of the pump, as a function of $N_{\perp} = k_{\perp}c/\omega_o$ for collisionless plasma, i.e. assuming $v_{\alpha} = 0$, and for collisional plasma, with $N_{\parallel} = k_{\parallel}c/\omega_o = 10$, $\delta = 0$ and plasma parameters as in Tab. I or at higher density $n_e = 2.0 \cdot 10^{18} \text{ m}^{-3}$. We note that in the collisional case at higher density the peak value of γ is negative, indicating that no unstable modes are obtained with such parameters. At the different peak values of γ the corresponding value of ω is fixed, approximatively given by the ion-acoustic angular frequency $\omega = k_{\parallel}v_{th,i}$.

In Fig. 2 we show the typical behaviour of the maximum value of γ/ω_o with respect to n_{\perp} , as a function of the angle δ , for collisional plasma, with $n_{\parallel} = 7$ (left, stable modes) and $n_{\parallel} = 10$ (right, unstable modes). The peak value is obtained for $\delta = 0$, a result common to all the other cases examined.

The real and imaginary part of the zeros of the collisionless PDR, corresponding to the maximum values of γ (with respect to k_{\perp} and δ) are plotted in Fig. 3 as a function of N_{\parallel} . As a result, the real part of the low frequency modes, as expected, follows the dispersion relation $\omega = k_{\parallel}v_{th,i}$, which is typical of the ion-acoustic waves. These are heavily damped in the linear approximation, but are driven unstable by LH wave power injection. The growth rates of this instability increase with N_{\parallel} .

The effect of the collisions is shown in Fig. 4. The behaviour of the frequency vs. the parallel wavenumber is not affected by the introduction of the collisions in the kinetic model, and still follows the linear dispersion of the ion-acoustic waves as in the collisionless case. However, the collisions have a profound effect on the imaginary part of the solution of the PDR. For plasma and rf parameters of Table I, unstable modes can exist only above a threshold value $N_{\parallel,th} \approx 7.5$. A simple physical interpretation of this result is that the collisions tends to maintain the distribution function close to the equilibrium, thus counteracting the nonlinear perturbation.

A parametric analysis of the solution of the PDR for different plasma and rf scenarios indicates that the collisions have, in general, a stabilizing effect. They can prevent the onset of the parametric instabilities and the amplification of LH sidebands up to relative large threshold values ($N_{\parallel,th} \geq 4$) of the parallel wavenumbers, within a wide set of plasma (near the LH antenna mouth) and rf parameters.

Scenarios at different plasma densities are considered in Fig. 5. In the collisionless case the role of the plasma density in determining the growth rates of the instabilities is marginal. However, the effect of the density is remarkable when the collisions are taken into account. We observe, at this regard, that the collisional frequencies are roughly proportional to the plasma density. As a result, the threshold value of N_{\parallel} for the onset of unstable modes is approximately proportional to the plasma density.

In Fig. 6 we compare two scenarios at different electron temperature, 5 eV and 6 eV. The results shown suggest a behaviour opposite to the collisionless case. The low frequency modes are most stable at lower temperature, as expected by the temperature dependence of the collisional rates, $\nu_e \sim T_e^{-3/2}$. We have observed that the effects of the collisions become negligible at temperature larger than 20 eV.

The stabilizing effect of the temperature ratio $\tau = T_i/T_e$ on PI is shown in Fig. 7. We note that the linear stability of the ion-acoustic quasi-modes increases with τ . Resonant ion-acoustic modes and strong PI are obtained for $\tau \ll 1$.

The stabilizing effect of the ion mass, predicted by a full wave analysis of the PI [25], is confirmed by the numerical solutions of the PDR derived here. In Fig. 8 the growth rates as a function of N_{\parallel} are plotted for different ion species. The growth rates of the PI in pure Lithium, single ionized plasma are much lower than in Hydrogen or Deuterium plasmas in both collisional and collisionless cases.

However, the threshold in N_{\parallel} for the onset of the PI, observed in the presence of collisions, is not significantly affected by the ion mass. Below this threshold, the lf mode are stable and their damping rates are larger for lighter ions.

Numerical solutions of the PDR with maximum value of γ , with respect to k_{\perp} and δ , have been found for different LH pump frequencies, namely 2.45 GHz, 3.7 GHz, 4.6 GHz, 5.0 GHz and 8.0 GHz. We assumed $N_{\parallel,o} = 1.8$, $n_e = 3 n_{e,cut-off}$, $T_e = T_i = 5 \text{ eV}$, and pure Deuterium plasmas. The power density considered for each frequency, given by $P(\text{kW/cm}^2) = 0.6 f_o(\text{GHz})$. The results, shown in Fig. 9, confirm the stabilizing effect of the collisions for each value of the pump frequency.

4. Discussion and conclusions.

A new parametric dispersion equation, including for the first time the effects of the collisions, has been derived in the frame of the kinetic theory to study the parametric instabilities induced by lower hybrid wave power injected in tokamak plasmas. A parametric analysis of the growth rates of the instabilities has been performed, comparing the results obtained using the collisional and collisionless kinetic models.

Several experimental scenarios have been considered, corresponding to LH antenna launchers operating in D plasma at 8.0 GHz, 5.0 GHz, 4.6 GHz, 3.7 GHz and 2.45 GHz, with power density that can be routinely transmitted by LH launchers at these frequencies. We have considered the operating frequency of the LHCD experiments in EAST (2.45 GHz and 4.6 GHz), JET and TORE SUPRA (3.7 GHz), FTU (8.0 GHz). 5.0 GHz is the LHCD operating frequency planned for ITER and DEMO. The main lobe of the power spectrum vs. the parallel refractive index has been assumed as located at $N_{\parallel} = 1.8$, which allow reasonable accessibility of the LH wave into the plasma core and efficient current drive in moderate density regimes, i.e. up to $n_{e,av} \sim 0.4 \cdot 10^{20} \text{ m}^{-3}$. As a result, for plasma densities at the antenna mouth given by three times the cut-off value, and electron temperature of 5 eV, the collisions significantly reduce the growth rates of the instabilities with respect to the collisionless case. Collisional suppression of PI occurs for a wide range of values of the parallel refractive index of LH sidebands, namely for $N_{\parallel} \leq N_{\parallel,th}$, where $N_{\parallel,th}$ is roughly proportional to the LH frequency. For the rf and plasma parameters considered $N_{\parallel,th} \approx 1.5 f_o(\text{GHz})$.

Increasing the plasma density near the antenna mouth, the stabilizing effect of the collisions becomes more important. This can be expected, since the collisional relaxation rate increases with the density. The threshold for the onset of the PI is approximately proportional to the plasma density. In collisionless case, instead, the effect of the density on the growth rates of the PI is marginal.

The effect of the electron plasma temperature is opposite in the collisional and collisionless model of PI. At lower T_e the stabilizing effect of the collisions becomes more important. In the collisionless model a reduction of the temperature results in larger growth rates of the PI. The collisions set a lower bound of the electron temperature for significant PI, which is of the order of 10 eV. Increasing T_e above 20 eV, the role of the collisions becomes marginal. The collisional relaxation rates indeed reduce as $\nu_e \sim T_e^{-3/2}$.

For larger electron temperatures, i.e. for $T_e > 100 \text{ eV}$, the effect of the collisions is completely negligible, but the nonlinear perturbation parameter $\varepsilon^2 \sim T_e^{-1}$ becomes so small that the PI are suppressed [21].

It has been also pointed out the role of the temperature ratio $\tau = T_i/T_e$ as well as the plasma composition on PI. The growth rates of the PI reduce increasing τ and the mass of the plasma ions, as predicted by the collisionless model [25].

However, the threshold value $N_{\parallel,th}$ does not change significantly for different ion masses, and an increase of the ion charge produces a strong increase of the growth rates.

The results above summarized are important for LHCD modeling of present experiments and for the design of the LHCD system in fusion reactors.

In present experiments, mainly if the rf power coupling occurs in a sort of cold and relative dense ($n_e \geq 2-3 \text{ } n_{e,\text{cut-off}}$) private plasma, the expected electron temperatures can be as low as a few eV. In such conditions, strong PI is always expected following the standard theoretical model. Taking into account the effects of the collisions, PI suppression might occur, and, in any case, significant growth rate reduction is predicted for the unstable modes. Gas injection, commonly used to achieve reliable coupling of LH waves [28, 29], decreases the electron temperature in front of the antenna mouth. Following the collisionless model, this should produce a strong increase of the PI with consequent large spectral broadening and peripheral rf power absorption. However, the gas injection technique does not reduce the LHCD performance, unless the gas injection is massive and produces a strong perturbation of the SOL. The stabilizing effect of the collisions provides a qualitative interpretation of these experimental results, since the collisions prevent large spectral broadening during moderate gas injection and operating at low electron temperature in front of the antenna mouth.

Concerning the application in fusion reactors, we observe that the LHCD antennas should be located in the shadow of the port, where the rf power coupling is expected to occur within a cold, private plasma. As a main result of the present analysis, we have found that collisional suppression of PI in such conditions allows such robust and safe design. Operating with sufficient high gradients of density and temperature, the amplification of LH sidebands around the main lobe of the N_{\parallel} power spectrum can be prevented, due to the enhanced convective losses and the narrow radial range of amplification. Operation in plasmas with high concentration of Lithium ions could be also considered, due to the stabilizing effect of ${}^6\text{Li}^+$ or ${}^7\text{Li}^+$ species. However, double ionization of Li atoms might occur in the temperature range (10-100 eV) where PI are expected, thus increasing the growth rates of such instabilities.

References

- [1] N. J. Fisch, *Phys. Rev. Lett.* **41** (1978) 873
- [2] N. J. Fisch, *Rev. Mod. Phys.* **59** (1987) 175
- [3] R. Cesario, et al., *Nature Comms*, **1** (2010) 55
- [4] J. Freidberg, 2007 *Plasma Physics Fusion Energy* (Cambridge: Cambridge University Press)
- [5] A. Cardinali, et al., submitted to *Nature Comms*.
- [6] R. Cesario and A. Cardinali, *Nucl. Fusion* **29** (1989) 1709
- [7] T. H. Stix, *Phys. Rev. Lett.* **15** (1965) 878
- [8] C. F. Karney, *Phys. Fluids* **22** (1979) 2188
- [9] M. Porkolab, et al. *Phys. Rev. Lett.* **31** (1977) 230
- [10] C. S. Liu and V. K. Tripathi *Phys. Rep.* **130** (1986) 143
- [11] R. Cesario and V. Pericoli-Ridolfini, *Nucl. Fusion* **27** (1987) 435
- [12] Y. Takase, et al., *Phys. Fluids* **28** (1985) 983
- [13] S. Bernabei, et al., *Phys. Rev. Lett.* **49** (1982) 1255
- [14] L. Chen and R. L. Berger, *Nucl. Fusion* **17** (1977) 779
- [15] Y. Takase, et al., *Phys. Rev. Lett.* **53** (1984) 274
- [16] C. Castaldo, et al., *Phys. Letters A* **230** (1997) 336
- [17] R. Cesario, et al., *Phys. Rev. Lett.* **92** (2004) 175002
- [18] R. Cesario, et al., *Nucl. Fusion* **46** (2006) 462
- [19] M. Brambilla, *Nucl. Fusion* **16** (1976) 11
- [20] F. De Marco, 1985 *Course and Workshop on Applications of RF waves to Tokamak Plasmas* (Varenna, Italy) ed S Bernabei et al (International School of Plasma Physics) p 316
- [21] R. Cesario, et al., *Nucl. Fusion* **54** (2014) 043002
- [22] J. M. Greene *Phys Fluids* **16** 2022 (1973)
- [23] M. Opher, G. J. Morales and J. N. Leboeuf, *Phys. Rev. E* **66** 016407 (2002)
- [24] B. A. Trubnikov, *Reviews of Plasma Physics*, Vol I (Consultant Bureau, New York, 1965) p. 105
- [25] F. Napoli, et al., *Plasma Phys. Contr. Fusion* **55** (2013) 095004
- [26] A. Zhao, Z. Gao, *Nucl. Fusion* **53** (2013) 083015
- [27] L. M. Delves and J. N. Lyness, *Math. Comp.* **21** (1967) 543
- [28] V. Pericoli Ridolfini, et al., *Plasma Phys. Control. Fusion* **46** (2004) 349
- [29] A. Ekedahl, et al., *Nucl. Fusion* **45** (2005) 351

f	Power density	$N_{ 0}$	Te	n_e	Composition	Te/Ti
8.0 GHz	3.5 kW cm ⁻²	1.8	5.0 eV	1.5 10 ¹⁸ m ⁻³	100% D	1.0

Table 1. Reference plasma and rf parameters for PI analysis. We have considered the power density that can be routinely coupled in FTU, corresponding to about 30% the maximum value which can be transmitted by a LH grill at 8.0 GHz.

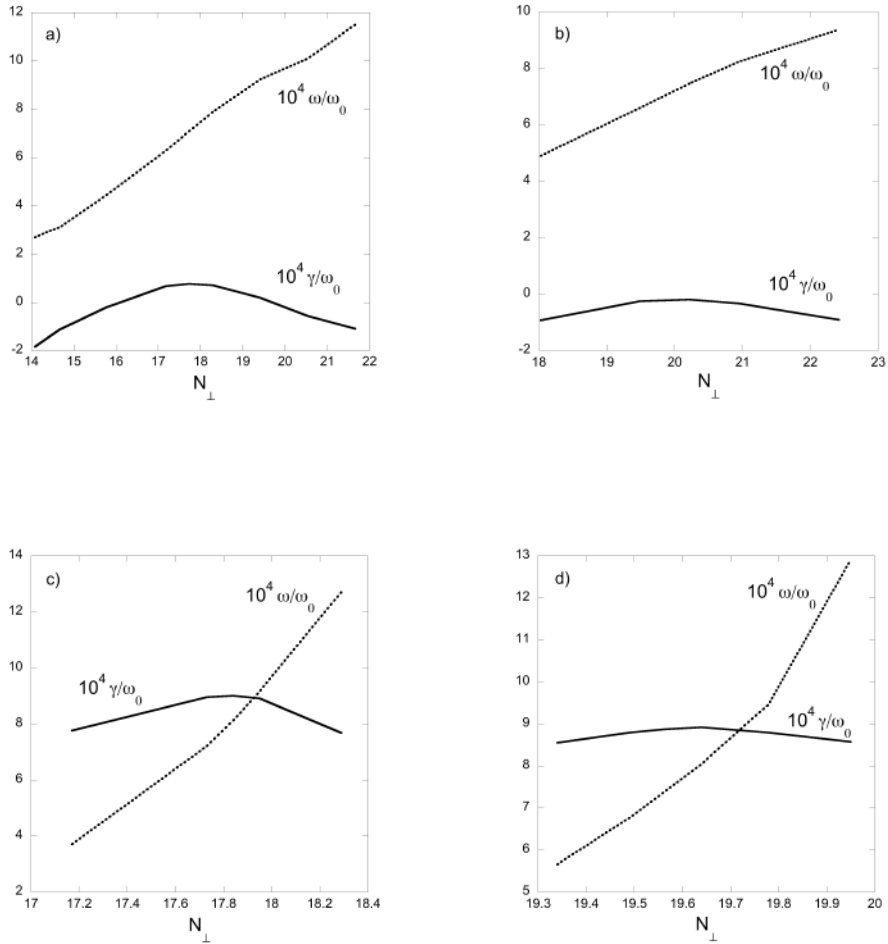


Fig.1 Numerical values of ω (dotted lines) and γ (continuous lines) normalized to the angular frequency of the pump, as a function of $N_\perp = k_\perp c / \omega_0$ for collisionless (a, b) and collisional (c, d) plasma, with $N_{||} = k_{||} c / \omega_0 = 10$ and $\delta = 0$. The plasma and rf parameters are as in Tab I in a) and c) plots, higher plasma density $n_e = 2.0 \times 10^{18} \text{ m}^{-3}$ is considered in plots b) and d).

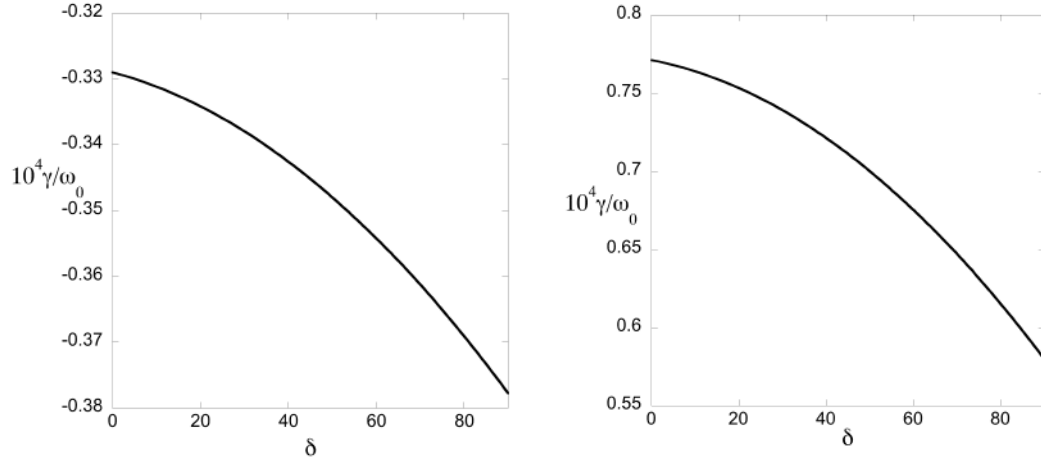


Fig. 2. The maximum value of γ/ω_o , with respect to n_{\perp} , is plotted as a function of the angle δ (in degrees) in collisional plasma for $n_{\parallel} = 7$ (left, stable modes) and $n_{\parallel} = 10$ (right, unstable modes). Reference parameters as in Tab. I.

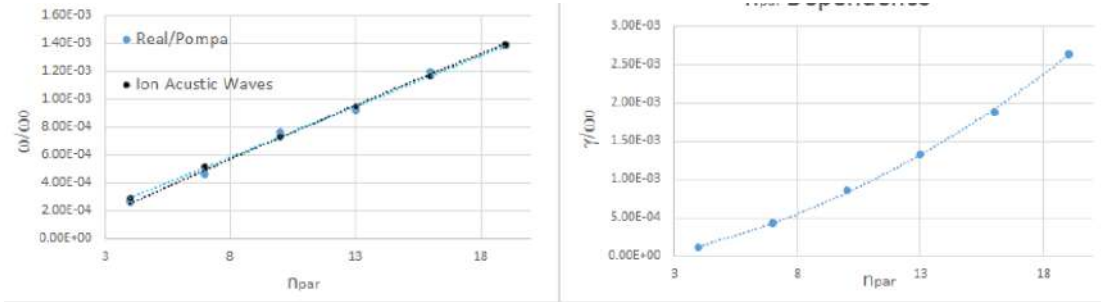


Fig. 3 The real and imaginary part of the zeros of the collisionless PDR, corresponding to the maximum values of γ (with respect to k_{\perp} and δ) plotted as a function of n_{\parallel} . The real part of the low frequency modes (left) follows the dispersion relation $\omega = k_{\parallel} v_{th,i}$, typical of the ion-acoustic waves. The modes are driven unstable ($\gamma > 0$, right) and the growth rates increase with n_{\parallel} . Reference parameters as in Tab I. (da rifare con le dens piu' basse)

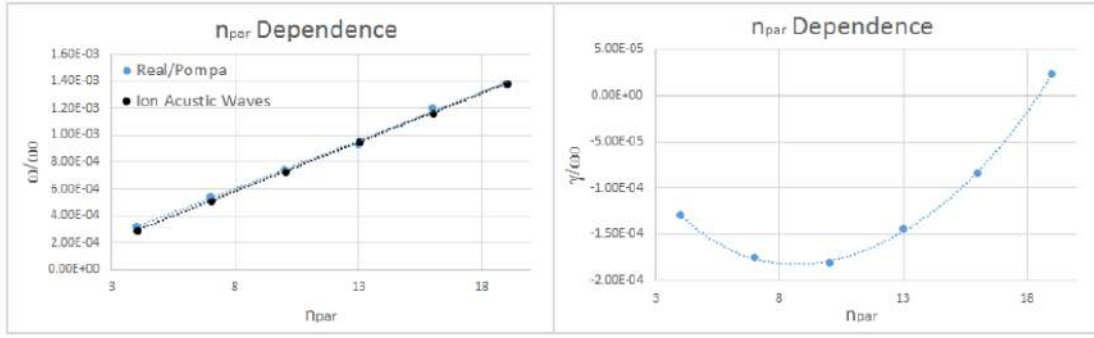


Fig. 4 Real and imaginary part of the zeros of the collisional PDR, corresponding to the maximum values of γ (with respect to k_{\perp} and δ) plotted as a function of n_{\parallel} . The behaviour of the frequency vs the parallel wavenumber (left) is not affected by the introduction of the collisions in the kinetic model, and still follows the linear dispersion of the ion-acoustic waves as in the collisionless case. Unstable modes (right) can exist only above a threshold value $n_{\parallel,th} \approx 18.5$, and the growth rates are orders of magnitude lower than in the collisionless case. (da rifare) bassi n_{\parallel} effetto nonlineare sparisce si va agganciare a $\text{elf}=0$ bassa frequenza lineare.

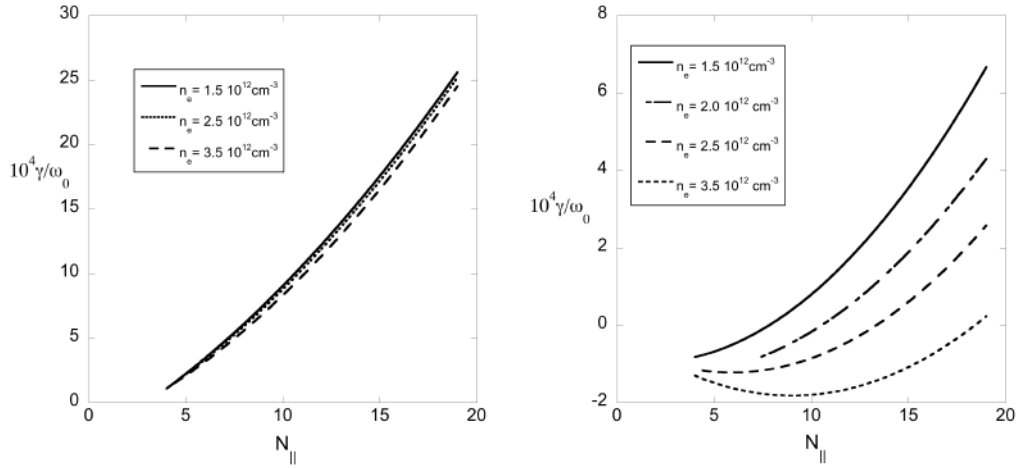


Fig. 5. Growth and damping rates at different plasma densities, with other rf and plasma parameters as in Tab I. In the collisionless case (left) the role of the plasma density in determining the growth rates of the instabilities is marginal. A stabilizing effect of the the plasma density is observed (right) when the collisions are taken into account.

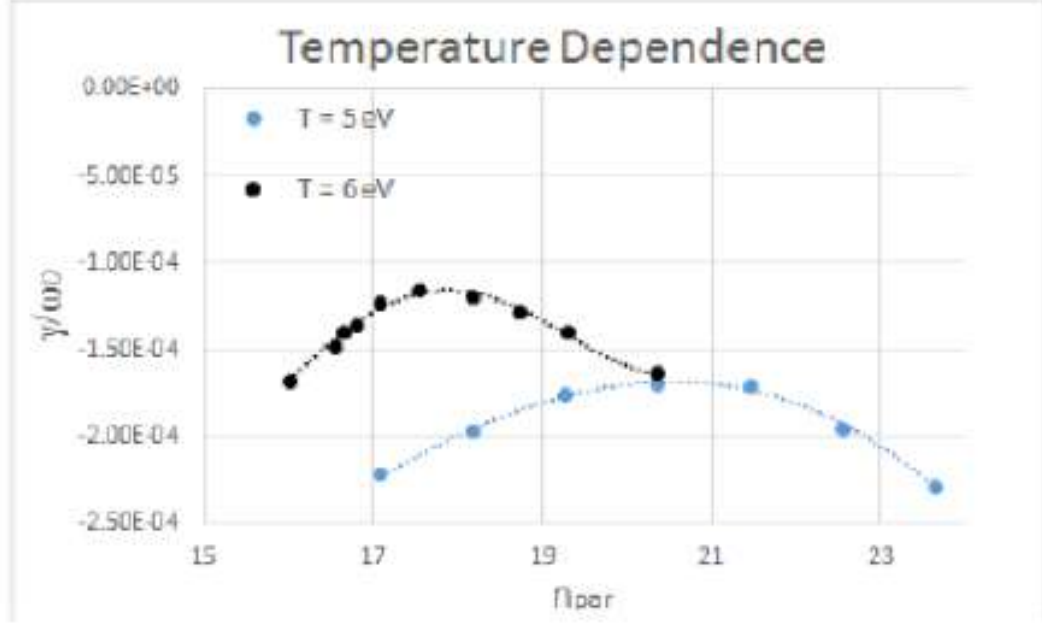


Fig. 6. Damping rates in two scenarios at different electron temperature, 5eV and 6 eV for collisional plasmas. The results shown suggest a behaviour opposite to the collisionless case. The modes are most stable at lower temperature.

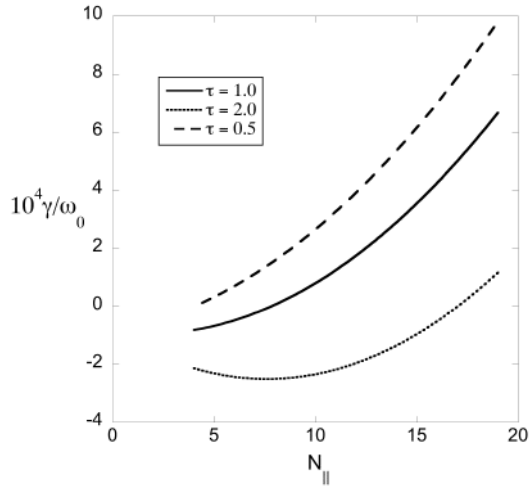


Fig. 7. Stabilizing effect of the temperature ratio $\tau = T_i/T_e$ on PI in collisionless (left) and collisional (right) plasma with rf and plasma parameters as in Tab. I.

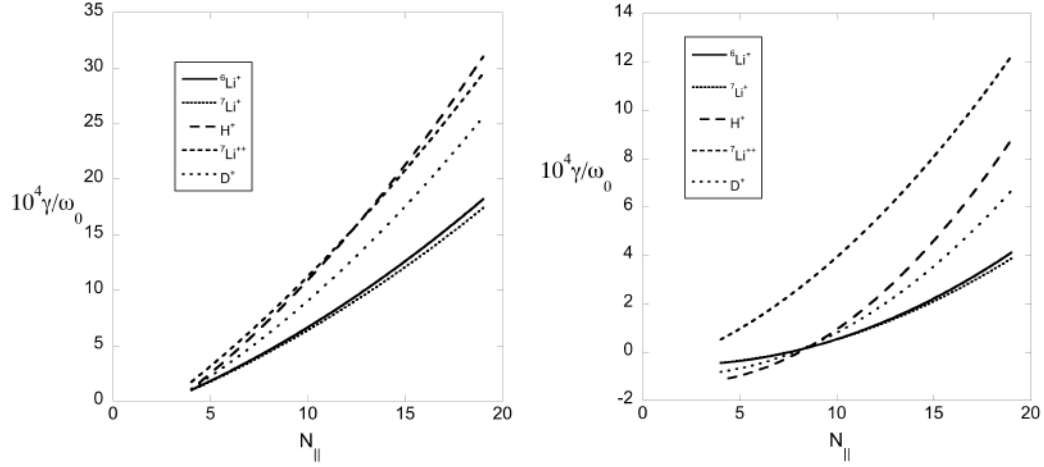


Fig. 8. Normalized growth rates γ/ω_0 vs N_{\parallel} for collisionless (left) and collisional (right) plasmas of different ion species, with plasma and rf parameters as in Tab. I. A significant reduction of the growth rates is predicted operating in plasmas of pure Lithium, single ionized, compared to Hydrogen or Deuterium plasma. In collisional plasmas, no unstable modes occur for $N_{\parallel} < 8.5$ and the damping rates are larger for lighter ions. Strong PI are always expected in double ionized Lithium plasmas.

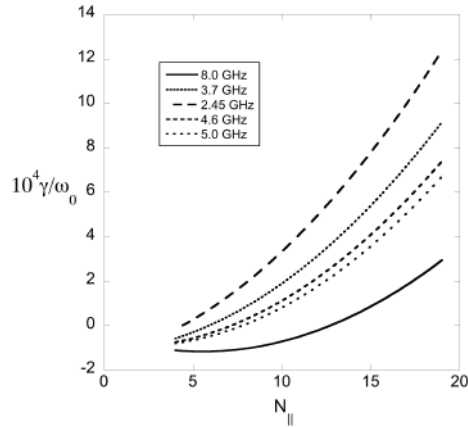


Fig. 9. Growth rates and damping rates of LH sidebands for different frequencies of the LH pump waves in collisionless (left) and collisional (right) D plasmas, with $n_e = 3 n_{e, cut-off}$, $T_e = T_i = 5$ eV, $N_{\parallel,0} = 1.8$ and power density given by $P(\text{kW/cm}^2) = 0.6 f_o(\text{GHz})$. A stabilizing effect of the collisions is expected for any value of the pump frequency.